Pharmaceutica Analytica Acta

Sunitha et al., Pharm Anal Acta 2017, 8:1
DOI: 10.4172/2153-2435.1000529

Research Article Open Access

Fabrication of Surgical Sutures Coated with Curcumin Loaded Gold Nanoparticles

Sunitha S[1*], Adinarayana K[1], Sravanthi Reddy P[1], Sonia G[1], Nagarjun R[1], Pankaj T[1], Veerabhadra Swamy Ch[1] and Sujatha D[1]

[1]*Department of Pharmaceutics, National Institute of Pharmaceutical Education and Research (NIPER-HYD), Balanagar, Telangana, India*

[2]*Institute of Pharmaceutical Technology, Sri Padmavathi Mahila Visvavidyalayam, Tirupati, Andhra Pradesh, India*

[*]**Corresponding author:** Sunitha S, Assistant Professor, Department of Pharmaceutics, NIPER-Hyderabad, Balanagar, 500037, Telangana, India, Tel: 0172 221 4687; E-mail: sunithaniper16@gmail.com

Received date: November 23, 2016; **Accepted date:** January 06, 2017; **Published date:** January 09, 2017

Abstract

Sutures are biomaterials regarded as a major cause of Surgical Site Infections (SSIs). Present work aims at a novel strategy to reduce nosocomial infections by coating sutures with antimicrobial drugs. Gold nanoparticles (GNPs) coated with antimicrobial drugs are well known for their antimicrobial activity. Hence, synthesis of gold nanoparticles by chemical reduction method followed by preparation of curcumin pegylated GNPs (CPGNPs) were carried out. The formation of the gold nanoparticles, thiolated gold nanoparticles (PGNPs) and CPGNPs was characterized by UV-Vis absorption spectroscopy, Fourier Transform Infrared Spectroscopy (FT-IR) and Scanning Electron Microscopy (SEM) techniques. The average particle size and polydispersity index of drug conjugated gold NPs were found to be 147.8 ± 2.03 nm and 0.286 respectively. The plain sutures (purchased from local market) were coated with curcumin pegylated GNPs by dipping technique and characterized by SEM to ensure the coating of curcumin conjugated gold nanoparticles on plain sutures. The CPGNPs coated sutures were evaluated for mechanical properties, drug release studies, biocompatibility, haemo-compatibility, sensitization and for *in vivo* studies. Histopathology was also done to study the effect of coated sutures on inflammation and cell repair at the site of surgery. The optimized coated sutures exhibited sustained drug release for 4 days and the antibacterial activity of the coated sutures was noticed in comparison to the uncoated sutures. From *in vivo* studies, it was clearly evident that coated sutures healed the tissue much faster than the uncoated sutures and less inflammation was observed. The same was concluded by the histopathology reports. The successful designing and development of drug-coated biodegradable sutures highlight the applicability of novel technique of coating for effective reduction of SSIs during the hospital stay.

Keywords: Biocompatibility; *Escherichia coli*; Nano-biotechnology; Nanomicelles

Introduction

Recent advances in the area of biomaterials have revolutionized the field of tissue engineering and regenerative medicine. Sutures are biomaterials widely used in wound closure with an aim to ligate injured blood vessels and to draw divided tissues together in clinical settings [1,2]. At present medical-surgical market is splendid with a large number of suture material which is different with reference to composition, tensile strength, structure, origin, type of absorption, treatment or purpose and is available in different sizes and indications. Several parameters like tensile strength, breaking strength, elasticity and capillarity are among important physical characteristics of sutures [3]. Depending on origin sutures can be broadly classified as natural or synthetic with degradation time varying from 60 days for absorbable sutures and longer for non-absorbable sutures [4,5]. Structurally they can be multifilament or monofilament with different resistance and flexibility [6-9].

Surgical site infections (SSIs) are the most common nosocomial infections that occur during long hospital stay [10]. According to national nosocomial infections surveillances system *Staphylococcus aureus*, coagulase-negative *staphylococci*, *Enterococcus* spp. and *Escherichia coli* are among the most frequently isolated pathogens at surgical sites [11]. Sutures are mainly responsible for approximately 23% of SSIs due to bacterial adherence and colonization in clinical settings with 5 fold increase in cost and extent of hospital stay by 20-fold [12]. Most of the commercially available sutures do not possess antimicrobial activity; this is where biomaterials with antibacterial property have been investigated by many research groups [13-15]. Vicryl Plus was the first marketed antimicrobial suture approved by the US FDA [16] but there are constant concerns that triclosan, when used as a coating agent, could lead to bacterial resistance and side effects due to its systemic absorption. One of the ways to prevent SSIs is by impregnation or coating the sutures with antimicrobial agents simultaneously taking care of prevention of bacterial resistance [17].

Coating with polymers is based on grafting the polymer functional groups such as carboxyl and attaching antibacterial agent. This suffers from problem of reduction in the mechanical properties of sutures. Among natural polymers chitosan and alginates are well explored for wound treatment with antibacterial and antifungal activity [18,19]. Coating sutures with natural antimicrobials in the form of nanoparticles can prevent the formation of bacterial colonies without compromising the mechanical properties. One of the promising approaches to overcome bacterial resistant infections is by using of metallic nanoparticles [20]. Reports are available in the literature to coat sutures with silver nanoparticles since it is found to have antibacterial property [21,22]. Gold nanoparticles (GNPs) have attracted significant interest as a novel platform for various applications such as nano-biotechnology and bio-medicine as they

offer convenient surface bioconjugation with molecular probes and remarkable plasmon-resonant optical properties.

Colloidal GNPs represents a completely novel technology in the field of particle based targeted drug delivery. The property of GNPs to bind proteins and molecules without altering their activity has given rise to their use in immuno-diagnostics as well as in histo-pathology. Owing to the small size and higher surface-to-volume ratio, makes GNPs to have better contact with microorganisms and increases the biological, chemical activities associated with high antibacterial activity [23]. Therefore, combining or conjugating antibiotics with GNPs increases the concentration of antibiotics at the infection site.

Hence, coating sutures with natural antibiotics which release drug in a controlled way can be quite useful against SSIs. Curcumin, a natural polyphenolic compound, obtained from Curcuma longa (turmeric) has many therapeutic applications with wound healing as a major advantage [24,25]. Preclinical trials have demonstrated low toxicity of curcumin even when used at relatively high doses. The main drawback of curcumin is lack of bioavailability because of low water solubility. Approaches like nanoparticles [26,27] liposomes, nanomicelles [28], phospholipids complexes [29] were used to improve the bioavailability of curcumin [30]. Manju and Sreenivasan reported the synthesis of GNPs of curcumin using polymer for conjugation to deliver to cancer cell [31]. But it was observed that upon conjugation the drug was less bioavailable for its activity as an important therapeutic group of the drug was bound irreversibly with conjugating agent [30]. Hence it is necessary to see that during conjugation the activity of the drug is maintained and at the same time imparting multi-purpose qualities.

In this context, we reported a new protocol for the formation of curcumin conjugated GNPs using thiolated Polyethylene Glycol (PEG) as a drug carrier. Thiolated PEG was selected as polymer which aids in conjugating the drug with gold nanoparticles. The thiolated PEG-drug conjugates have an advantage of prolonged resistance in the body with decreased degradation by metabolic enzymes.

Hence, the present study made an attempt to design and develop curcumin loaded gold nanoparticles and their incorporation on the surface of the selected sutures to release the drug in a controlled manner for a long time. Evaluation of the coated sutures for their efficacy, safety, and stability using standard procedures were carried out for establishing scientific evidence for clinical use.

Materials and methods

Materials

Curcumin, poly (ethylene glycol) methyl ether thiol (mol.wt 2000), sodium alginate, aurochloric acid (HAuCl4) and sodium tetra borohydride were purchased from Sigma-Aldrich. TRUGLYDE FAST-absorbable surgical suture U.S.P (Synthetic), Polyglycolic acid sutures were procured from local market. *Escherichia coli*, *Staphylococcus aureus* were purchased from NCCS, Pune. Dialysis membrane (M.W cut off 12000 to 14000), agar and trypticase soya broth were purchased from Himedia. All the glassware used for the synthesis was washed with aqua regia which is a mixture of nitric acid and hydrochloric acid. Then the glassware was rinsed with double distilled water followed by drying at 80-100°C in a tray dryer for 12 h. All other solvents were purchased from Sd fine chem Ltd.

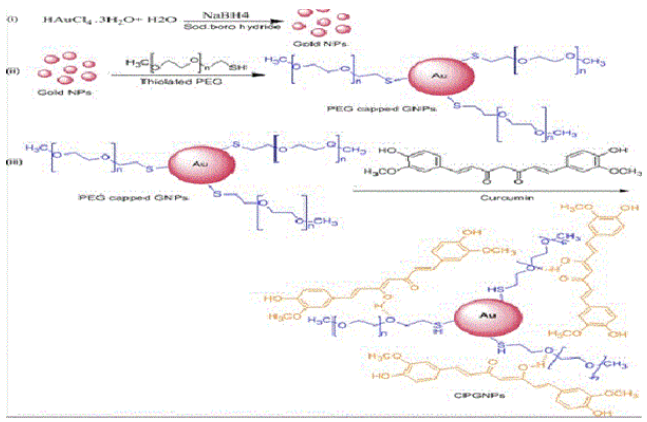

Figure 1: Scheme representing the synthesis of (i) Gold nanoparticles (GNPs), (ii) Pegylated GNPs and (iii) Curcumin conjugated PGNPs (CPGNPs).

Synthesis of gold nanoparticles (GNPs), Pegylated GNPs (PGNPs) and Curcumin pegylated GNPs (CPGNPs)

Briefly, 1 mL of 5 mM aurochloric acid solution was boiled and stirred on a magnetic stirrer (REMI) for 1 h at 300 rpm. An aqueous 2 mM sodium tetra borohydride (reducing agent) was added drop wise to aurochloric acid solution with continuous heating (8-10 min) to complete the reaction which is manifested by color change (colorless to purple) indicating the formation of gold nanoparticles. The synthesis of GNPs was optimized by using different concentrations (mM) of aurochloric acid to concentrations of sodium borohydride (mM) at different processing conditions represented in Table 1. Prepared GNPs were coated with thiolated PEG as reported earlier by Jokerst, Leung and Veronese [32]. In brief for coating, thiolated polyethylene glycol solution (1% w/v) was added to synthesized GNPs at room temperature and stirred for 3 h for the formation of pegylated GNPs. The formed nanoparticles were centrifuged at 10000 rpm for 30 minutes to remove unreacted polymer and redispersed the sediment in distilled water (10 ml). Coating of poly (ethylene glycol) methyl ether thiol was confirmed by measuring the UV-Vis absorbance at 541 nm supported by its plasmon resonance mechanism of metallic nanoparticles. For CPGNPs synthesis 2% w/v of drug solution (acetone) was added to 50 mL PGNPs solution under magnetic stirring for 3 h at room temperature. The formed CPGNPs were separated by centrifugation at 1000 rpm for 30 min to remove unattached drug. The final solution was freeze dried and used for further analysis.

Coating of CPGNPs onto sutures

Coating of CPGNPs onto the sutures is done by the slurry dipping technique with the use of sodium alginate as an immobilizing agent. Accurately, 10 mL of 2% w/v sodium alginate was added to 10 mL of 0.1% w/v sodium chloride (NaCl) under magnetic stirring for 8 h at room temperature. CPGNPs (10 mg/mL) were added to above mixture with stirring for 30 min for the formation of alginate-curcumin gold colloidal nanoparticles.

Sutures of length 2 cm were dipped in the formed alginate-curcumin gold colloidal NPs solution for 10 min followed by air drying for 5 min. The above process was repeated 10 times for adequate

coating of the sutures. For cross-linking coated sutures were immersed in 4% w/v calcium chloride solution and kept for 30 min to ensure complete cross-linking followed by washing with double distilled water [12].

The percentage of drug coating onto the sutures was calculated by using the below formula:

$$Wt\% = \frac{(W2 - W1) \times 100}{W1}$$

Where W1: Weight of uncoated suture, and W2: Weight of coated suture.

Characterization

The synthesized GNPs, PGNPs and CPGNPs were characterized by UV-Vis spectrophotometry (V 650, Jasco) and FT-IR (Perkin Elmer).

UV-visible and FT-IR spectroscopy

The maximum absorbance of gold nanoparticles, PEG-coated gold nanoparticles, curcumin gold nanoparticles were identified by measuring the plasmon resonance of metallic nanoparticles in the range of 200-800 nm. An FT-IR spectrometer was used for obtaining spectra in the range of 400-4000 cm^{-1}.

Particle size, polydispersity index (PdI) and zeta potential (ZP)

The particle size, PdI and zeta potential were measured using Zeta sizer (Malvern ZS90, UK). High ZP indicates stabilization of prepared formulation and positive charge which attract the negative charge of skin. Hence increasing the contact time of drug thereby increases the therapeutic activity of the drug.

Scanning electron microscopy (SEM) analysis

Morphological characterizations of synthesized nanoparticles were visualized using SEM (SEM-S-3700N). Samples were prepared by dropping the nanoparticles dispersion on an aluminum stub and air dried at room temperature.

Entrapment efficiency (EE) and drug release

For EE 5 mg of freeze-dried CPGNPs were dissolved in 10 mL of phosphate buffer pH 7.4 and bath sonicated for 15 min to completely dissolve the drug. After filtration and suitable dilution, the drug concentration was determined by UV-Vis spectrophotometer at 431 nm and EE was calculated using the given formula.

Entrapment efficiency=Amount of drug in NPs/Total amount of drug × 100

The release of curcumin from coated sutures was estimated by performing immersion studies. Coated sutures were placed in cotton plugged sterile conical flask containing 50 mL of simulated body fluid (SBF) solution of pH 7.4 and kept on a magnetic stirrer at room temperature. Samples were withdrawn at respective time intervals (12, 24, 36, 48, 60, 72, 84, 96) h and analysed for drug content using UV-visible spectroscopy at 431 nm [12,33].

Stability

To determine the stability of the curcumin molecules bound to the surface of GNPS the functionalized NPs were stored for more than 4 weeks as per ICH storage conditions and monitored for particle size, PdI and EE.

Measurement of mechanical properties

The diameter of the plain sutures and coated sutures were measured using a micrometer at different positions of the sutures and an average diameter of the suture was calculated and expressed in millimeter.

An important property of the suture is its tensile strength as it helps the practitioner to make a knot. If the suture is very weak by applying high knotting force the suture may break very easily. Hence, it is very important to determine the tensile strength of the coated suture. Mechanical properties like Tensile Strength (TS), and elongation at break (E/B) were evaluated using ultra test, mecmesin, UK set with 25 kg load cell with minor modifications. Coated suture of 8 cm length was taken and fixed between two clamps which were positioned at a distance of 3 cm and the strips were pulled with top clamp at a rate of 1 mm/s till the film breaks.

The mechanical properties were calculated using the below formulae [34]. These properties were evaluated to confirm the physical quality of the coated sutures in terms of strength and physical stability.

$$\text{Tensile strength (kg. mm}^{-2}) = \frac{\text{Force at break (kg)}}{\text{Initial cross sectional area of the sample (mm}^2)}$$

$$\text{Elongation at break (\% mm}^{-2}) = \frac{\text{Increase in length (mm)}}{\text{Original length (mm)}} \times \frac{100}{\text{Cross sectional area}}$$

Antibacterial assay

The antibacterial assay was performed on non-pathogenic *Escherichia coli* (*E. coli*) and *Staphylococus aureus* (*S. aureus*) for curcumin coated sutures and uncoated suture (control). Inoculums (100 µL) of fresh cultures were spread on to nutrient agar medium (NAM) plates. The CPGNPs coated sutures and uncoated sutures of length 2 cm were placed in petri plates after inoculation. The plates were incubated at 37°C for 24 h and zone of inhibition was measured after 48 h. The assay was performed in triplicates.

Haemocompatibility studies

Haemocompatibility testing of medical devices was performed by total haemolysis test as described according to practice F756-08 [35] using human erythrocytes and the test was performed with isotonic extract of the test material in contact with human blood as described in practice F619-03 [36].

In brief, the coated sutures and uncoated sutures of 2 cm each were incubated in normal saline for 24 h in Biological Oxygen Demand (BOD) incubator at 37°C. After 24 h of incubation, the sample extracts were taken as a test with 0.1% w/v sodium carbonate as a positive control and normal saline of pH 7.2 (0.9% w/v Sodium chloride) as a negative control. For haemolysis testing, fresh 200 µL diluted blood was mixed with each test sample, positive control and negative control. These samples were then incubated for 3 h at 37°C followed by centrifugation to remove any solid particles.

The samples were then read at 540 nm using ELISA reader and the % of haemolysis was calculated as per the following formula [37,38].

$$HP(\%)\frac{(D_T - D_C)}{(D_{PC} - D_{NC})} \times 100$$

Where D_t: Absorbance of test, D_c: Disease control, D_{pc}: Absorbance of positive control, D_{nc}: Absorbance of negative control.

Cytotoxicity studies

Cytotoxicity of the coated sutures was evaluated using MTT 3-(4, 5-dimethylthiazol-2-yl)-2, 5-diphenyltetrazolium bromide survival assay [39]. The test sample for cytotoxicity test was prepared according to ASTM standard F619–03. The two different test materials uncoated marketed suture (control) and CPGNPs coated sutures were added separately in 10 mL Dulbecco's Modified Essential Media (DMEM) for 24 h at 37°C.

After incubation, the prepared media alone was used as a test sample. The 3T3-mouse embryo fibroblast cells were seeded (1.5×10^4 cells/well) in 96 well microtitre plates in triplicate and cultured in DMEM supplemented with 10% fetal bovine serum (FBS) containing sodium bicarbonate ($NaHCO_3$) (1.2 g/L) and penstrep antibiotic (0.025 g/L ampicillin, 0.1 g/L streptomycin) at 37°C in atmosphere of 5% CO_2.

Then, 100 µL test sample was added to media in triplicates along with fresh media (control). Finally, these samples were incubated for 24 h at 37°C. After incubation, MTT (5 mg/mL) was added to each well and the formazan crystals were dissolved by DMSO. The absorbance was read in a microtitre plate reader (ADD MAKE) at 570 nm, 30 min after the solubilization of the crystals. The percentage cytotoxicity was calculated by the formula:

Cytotoxicity = [(O. D of control–O.D of test)/O. D of control] × 100

Where O.D is Optical Density

In vivo studies

All the animal studies protocols were duly approved by the Institutional Animal Ethics Committee (IAEC) under protocol no NIP/2/2015/PE/132. Swiss albino mice of 20-30 g and 4-5 weeks old were supplied by the Teena labs, India.

The animals were acclimatized at a temperature of 25°C ± 2°C and relative humidity of 50-60% under natural light/dark conditions for one week before experiments. Mice were randomized into two groups (n=8).

After anesthesia with ketamine (50 mg/kg, i.p) and xylazine (5 mg/kg, i.m) laparotomy was done in mice with a 2 cm cut on ileum near ceacum with scissors. Intestinal defect was closed using single layered, interrupted anastomosis using uncoated and CPGNPs coated sutures in the two groups respectively. The abdominal wall was closed with running suture in both peritoneal-muscular layers and skin layer. All the techniques were performed in the sterile area. At the end of surgery, mice were allowed free access to water and a liquid diet.

At the end of day 7, ileum was excised from euthanized animals and observed for adhesion formation scores. The excised ileum samples were stored in formalin buffer until further evaluation of histopathology. The adhesion formation scores were done as per the scoring scale of Van der Ham et al. [40].

Briefly, on macroscopic observation at anastomotic site the score was given as follows: 0: No adhesions; 1: Minimal adhesions between anastomosis and omentum; 2: Moderate adhesions between omentum and anastomosis; and 3: Severe and extensive anastomosis including abscess formation.

The histopathological sections of ileum were scored for parameters like inflammatory cell infiltration and fibroblast growth as per the modified Ehrlich and Hunt numerical scale (0–4) under a light microscope and were scored in a blind fashion [41,42].

Results and Discussions

Synthesis of gold nanoparticles (GNPs), Pegylated GNPs (PGNPs) and Curcumin pegylated GNPs (CPGNPs)

In the present study GNPs were synthesized using 5 mM aurochloric acid to 2 mM sodium tetra borohydride as a metal precursor and reducing agents respectively (Table 1). The formation of GNPs was indicated by color change as shown in the Figure 2 [31].

S. No	$HAuCL_4$ (5 mM)	$NABH_4$ (2 mM)	Ratio	Size ± S.D	PdI ± SD
1	0.125	1	0.25:1	95 ± 4.04	0.312
2	0.25	1	0.5:1	132 ± 3.05	0.291
3	0.375	1	0.75:1	123 ± 2.88	0.245
4	0.5	1	1:1	79 2 ± 0.51	0.281
5	0.5	0.25	1:0.25	843 ± 0.05	0.372
6	0.5	0.5	1:0.5	104 ± 2.51	0.267
7	0.5	0.75	1:0.75	157 ± 2.52	0.381
8	0.5	2	1:2	123 ± 2.72	0.437
9	0.5	3	1:3	197 ± 3.2	0.341
10	0.5	4	1:4	243 ± 3.7	0.273
11	0.5	5	1:5	172 ± 2.1	0.675
12	1	1	2:1	64 ± 1.5	0.391
13	1.5	1	3:1	83 ± 2.5	0.243
14	2	1	4:1	97 ± 1.5	0.275
15	2.5	1	2:5	222 ± 2	0.632

Table 1: Data of optimization design for preparation of Gold NPs using different mM ratios of gold solution and sodium borohydride.

The formation of CPGNPs was carried out by a two-step process. In the first step PGNPs were synthesized by coating 1% w/v thiolated PEG to optimized gold nanoparticles on a magnetic stirrer at 300 rpm [32].

The coating of the thiolated polyethylene glycol was confirmed by measuring UV spectra followed by conjugation of curcumin to the PGNPs.

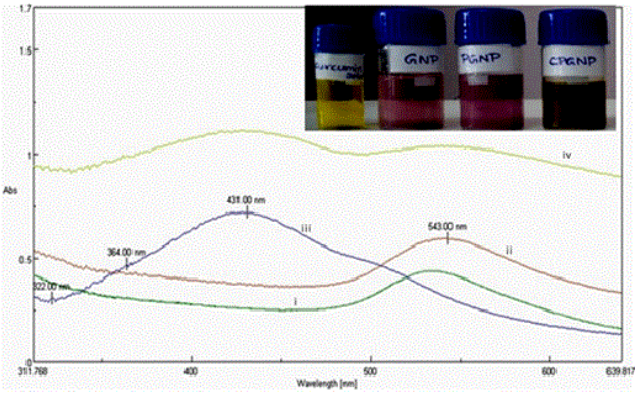

Figure 2: UV-Vis spectra of (i) GNPs, (ii) Thiolated PGNPs, (iii) Curcumin and (iv) CPGNPs.

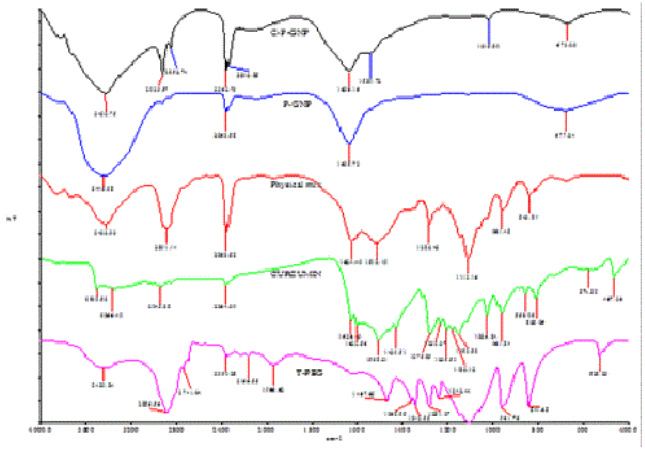

Figure 3: FT-IR spectra of (i) Thiolated PEG, (ii) Curcumin, (iii) Physical mixture, (iv) PGNPs and (v) CPGNPs.

UV-Vis and FT-IR spectroscopy

UV-Vis spectra of (i) GNPs,(ii) thiolated PGNPs, (iii) curcumin and (iv) CPGNPs in aqueous media were depicted in Figure 2. Curcumin shows an absorption peak at 431 nm which indicates basic di aryl heptinoid chromophore group. In case of blank GNPs maximum absorbance was seen at 541 nm which is the characteristic peak for gold nano particles. Absorption peak in spectra of thiolated PGNPs was seen at 364 nm (thiol group) and 543 nm which is a distinguishing peak of PGNPs arising due to surface plasmon resonance [43]. Curcumin functionalized PGNPs shows two distinct characteristic peaks at 436 nm and 550 nm which confirm the modified functional groups of components in the gold curcumin complex NPs. The increase in wavelength for absorption peak of curcumin by 5 nm and GNPs 7 nm may be ascribed to the conjugation of thiolated PEG functionalized GNPs with the drug.

The results of UV-Vis spectroscopy were also supported by FT-IR. Figure 3 depicts the FT-IR spectra of (i) thiolated PEG, ii) curcumin, iii) Physical mixture, (iv) thiolated PEG capped gold nanoparticles and v) thiolated PEG functionalized GNPs. The signatures of thiolated PEG may be recognized as C-H stretching (2886 cm^{-1}), CH bending (1360 cm^{-1}), C-O-C stretch (1000-1300 cm^{-1}). Signatures of curcumin are free OH (3503 cm^{-1}), CH aryl (3013 cm^{-1}), CH methyl (2943 cm^{-1}), C=O and C=C enol (1429 cm^{-1}-1630 cm^{-1}) and C-O-C (1000 cm^{-1}-1300 cm^{-1}) contributed by symmetric and asymmetric contributions of C-O-C chains [26]. Spectrum (iv) illustrates the functionalization of sodium borohydride reduced GNPs with thioPEG with a shift of CH stretch from 2359 cm^{-1} to 2363 cm^{-1}. Spectrum (v) clearly discloses the characteristic peaks of both thiolated PEG and curcumin. Drug molecules were attached to functionalized GNPs by intermolecular hydrogen bonding with a shift of OH stretching [30]. The basic heptinoid group of curcumin remains integral and negatively charged gold nanoparticles bind with SH group of polyethylene glycol in pegylated nanoparticles. Thus UV-Vis data with the support of FT-IR results confirms the formation of CPGNPs.

Coating of CPGNPs on sutures

Alginate represents a family of polysaccharides composed of homo polymeric region of β-D-mannuronic acid and α-L-guluronic acid interspersed with mixed sequences and has been widely used as an immunoisolation membrane for transplantation purposes [44] and as an immobilization agent for enzymes [45]. Hence, curcumin pegylated GNPs were immobilized before coating onto the sutures. Immobilization provides the inert and biocompatible system with resistance to high temperature with retained activity. The coating of alginate CPGNPs over sutures was done by a slurry dipping technique in the aseptic condition in laminar flow and the same was confirmed by SEM images, drug release studies and antibacterial assay.

Particle size, PdI and zeta potential

The particle size was measured by Malvern zeta sizer in double distilled water. The average particle size of GNPs is 64.80 nm ± 0.4 nm and the average diameter of PGNPs is 96.80 nm ± 2.6 nm with PdI 0.391 and 0.222 respectively. The average diameter of CPGNP is 147.8 nm ± 2.7 nm with PdIof 0.286. The results (Table 2) clearly an indicate an increase in particle size after conjugation of drug. Zeta potential was found to be -29.63 mV ± 0.45 mV which provides enough surface charge to stabilize particles from aggregation.

Formulation	Z-Average (d. nm)	PdI	ZP (mV)
GNPs	64.80 ± 1.54	0.391	-31.9
PGNPs	96.80 ± 1.89	0.222	-30.47
CPGNPs	147.8 ± 2.03	0.286	-29.63

Table 2: Particle size, PdI and ZP of optimized formulations.

To know the effect of different concentrations (mM) of gold to thiol, the PGNPs were synthesized at different ratios of gold to thiol and their effect on particle size and PdI were measured for which the data is shown in Table 3. From the results it was found that gold/thiol ratio of 2:1 resulted in particle size of 88 ± 0.34 nm with PdI 0.254. Hence it was selected for further studies.

Scanning electron microscopy

SEM analysis revealed morphological features of the prepared GNPs, PGNPs, CPGNPs, plain suture and coated suture. From Figure 4 it was found that the prepared GNPs and drug loaded nanoparticles possess spherical shape with a smooth surface without visible particle aggregation. SEM analysis of coated suture surface and plain suture surface clearly distinguish uniform coating of CPGNPs over suture (Figure 5). The surface of the coated sutures was rough indicating the coating of drug loaded CPGNPs [46]

Formulation Code	Gold /thiol polymer	Particle size (nm)	PdI	ZP	E.E (%)
GT1	1:2	168 ± 1.2	0.322	-31.9	60 ± 2
GT2	5:1	254 ± 0.31	0.435	-10.2	68 ± 3.60
GT3	1:1	154 ± 2.3	0.126	-19.8	70 ± 2
GT4	2:1	88 ± 0.34	0.254	-27.80	84 ± 2.52
GT5	2:5	167 ± 1.52	0.472	-29.3	55 ± 2.08

Table 3: Data of particle size and PdI with different concentration of gold to thiol ratio.

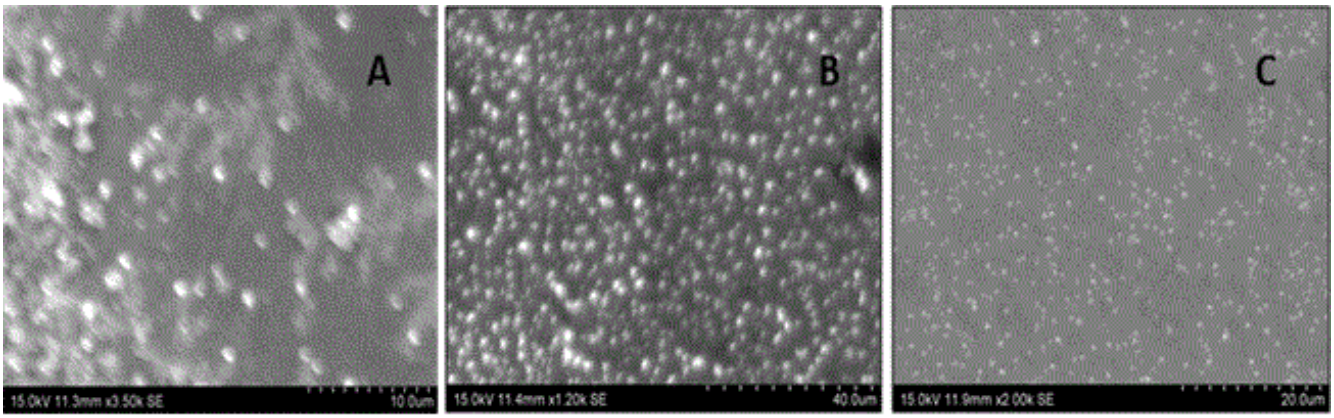

Figure 4: SEM images of (A) GNPs, (B) PGNPs and (C) CPGNPs.

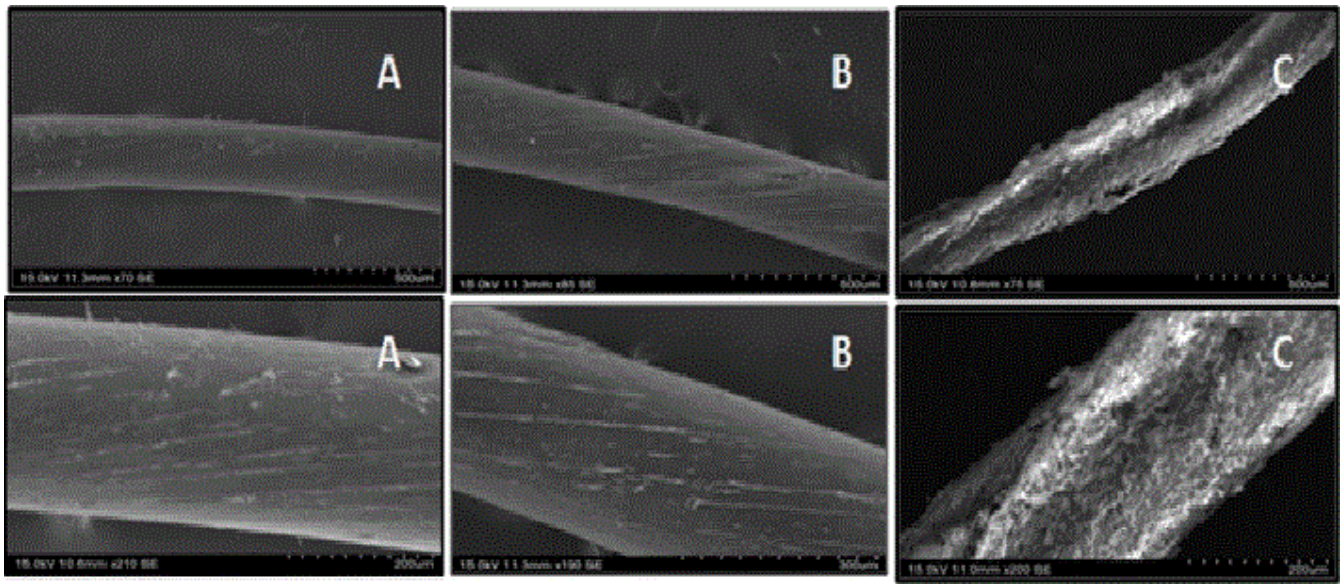

Figure 5: SEM images of (A) Plain suture, (B) Drug coated sutures and (C) CPGNPs coated sutures at different magnification.

Entrapment efficiency and drug release

The results of entrapment efficiency of drug loaded GNPS were shown in Table 3. Entrapment efficiency was ranging from 55% ± 2.81% to 84% ± 2.56% and highest entrapment was found when drug to thiolated PEG ratio was 2:1. High entrapment may be attributed to the attachment of two drug molecules to a polymer having two active sites. Hence, this ratio was further selected for coating onto sutures. The percentage drug release was studied in SBF and the release is shown in Figure 6. The drug was released from coated sutures up to 4 days.

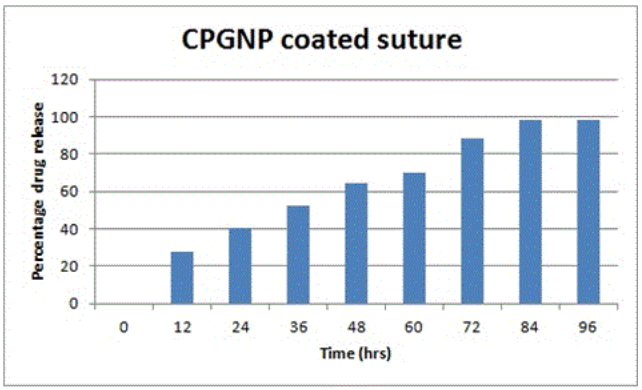

Figure 6: *In vitro* release of CPGNPs into SBF from coated sutures.

Stability studies

Stability studies were done as per ICH guidelines for CPGNPs for two months and monitored for particles size, PdI and entrapment efficiency. The nanoparticles when stored at 40°C ± 2°C, 75% ± 5% RH showed a slight increase in particle size from 147.8 nm ± 2.22 nm to 180 nm ± 3.68 nm and PdI changed from 0.286 to 0.88. The EE was decreased from 84 to 82% (Table 4).

From the studies it was found that stability of the drug conjugated gold nanoparticles was not affected even when stored at different conditions.

Measurement of mechanical properties

An important property of the suture is its tensile strength and mechanical properties as itdecides the ease with which the practitioner can make a knot. From the current study, the standard marketed suture was found to have a diameter of 0.370 mm ± 0.26 mm with a tensile strength of 3.90 kg/m^2 ± 0.156 kg/m^2 whereas the coated suture has a diameter of 0.0398 mm ± 0.31 mm with a tensile strength of 3.88 kg/m^2. The drug coating did not affect tensile strength of the suture. There was no significant difference in the elongation at break which was around 32.37% ± 2.46% for uncoated suture and around 30.64% ± 3% for drug-coated suture. From the results, it is clear that coating did not affect the tensile strength and elongation at break of the suture, indicating no prominent alterations of the mechanical properties of the coated sutures.

Formulation code	Storage conditions	EE		Particle size		PdI	
		Initial (%)	Final (%)	Initial (nm)	Final (nm)	Initial	Final
GT4 (2:1)	25°C ± 2°C, 60 ± 5% RH	84	78	147.8	265.9	0.286	0.711
	40°C ± 2°C,75 ± 5% RH	84	82	147.8	180	0.286	0.88
	2-8°C	84	80	147.8	212.5	0.286	0.141

Table 4: Data of stability study.

Antibacterial assay

The main purpose of drug coating on to the suture was to inhibit the bacterial growth, thereby facilitating the healing and prevention of SSIs. The antibiotic diffuses out from the coated sutures and inhibits the growth of bacteria resulting in a zone of inhibition. The antimicrobial activity of the studied sutures using agar diffusion method has been represented in Figure 7 and the zone of inhibition values are tabulated in Table 5. Surrounding the CPGNPs coated sutures there was a clear zone of inhibition in both gram positive and negative micro organisms as compared to uncoated sutures.

Cytotoxicity studies

Cytotoxicity of the coated and uncoated sutures on $3T_3$-mouse embryo fibroblast cells using MTT assay the cytotoxicity of the different sutures has been mentioned in Table 5. The results revealed the biocompatibility of the coated sutures and fibroblast cells were viable up to 94.6% in CPGNPs coated sutures when compared to 95.8% with uncoated sutures. The observed preservation of cell viability can be attributed to not using any organic solvents in the process of preparation of NPs and their coating on sutures. Though acetone has been used in dissolving curcumin it has not shown any cytotoxicity in the cell cultures. Both haemocompatibility and cytotoxicity studies support the safety and biocompatibility of the coated sutures.

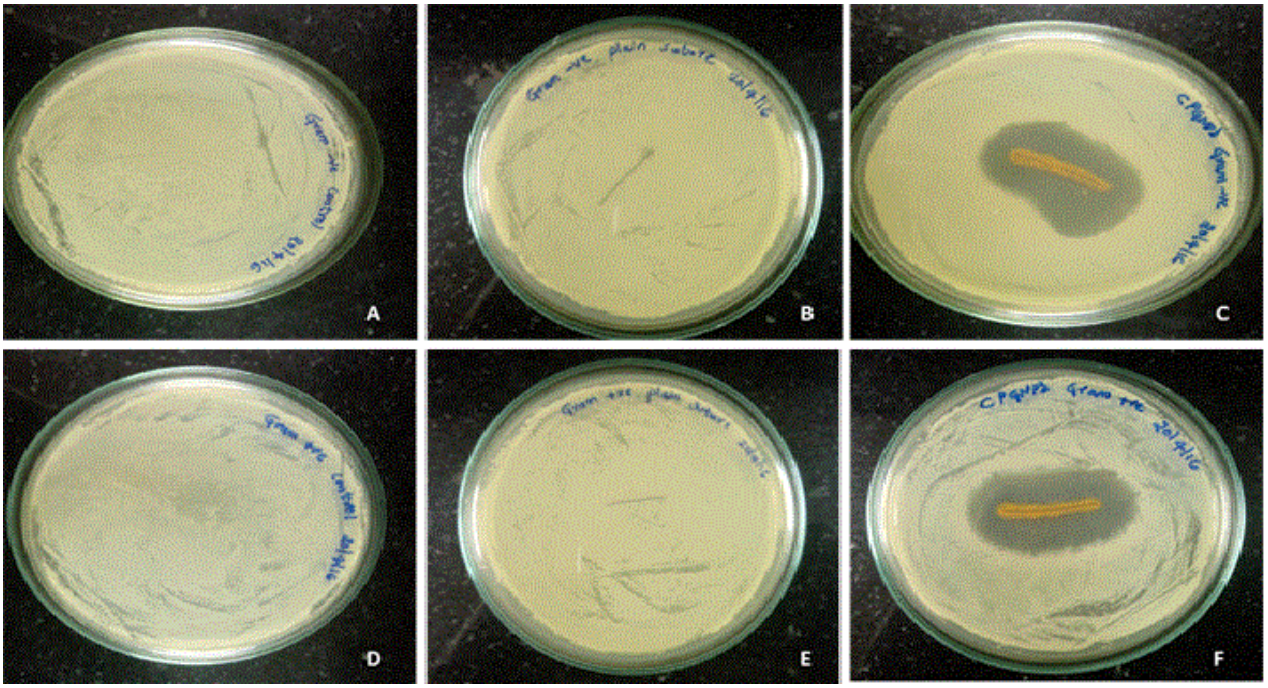

Figure 7: Antimicrobial activity of coated and uncoated sutures. a and d were control for gram -ve and gram +ve bacteria respectively, b and c shows effect of coated and uncoated sutures on gram -ve bacteria, e and f shows effect of coated and uncoated sutures on gram +ve bacteria.

Haemocompatibility studies

Haemocompatibility assay is considered to be a simple, reliable and reproducible method for estimating compatibility of biomaterials as per ASTM guidelines (ASTM; F 756–08). Based on their hemolytic index (hemolysis%) as per the guidelines materials were classified into three different categories. If the percentage of hemolysis is over 5% the material is considered as highly hemolytic; while the one with a haemolytic index between 5% and 2% are said to be slightly hemolytic and if hemolysis percentage is below 2%, the material is considered as a non-hemolytic material. This assay has been carried out to study the compatibility of coated sutures with blood cells and components as haemolysis by biomaterials is prime factor deciding their toxicity. The % hemolysis of different sutures has been tabulated (Table 5) and it was observed that the CPGNP scoated sutures falls in non-hemolytic category similar to that of uncoated sutures explaining their biocompatibility.

In vivo study

The *in vivo* studies were done and the images of the animals with coated sutures and their absorption after 7 days is seen in Figure 8 and the histopathology studies revealed that uncoated sutures have shown numerous thick adhesions around anastomosis whereas loose, minimal adhesions were found in both the groups sutured with coated sutures (Figures 8 and 9). Results of the *in vivo* intestinal anastomosis model have demonstrated better healing and less inflammation with coated sutures. The incidence of any pus, abscess and sepsis are not found in any of the experimental groups. The adhesion score is referred as an excellent macroscopic parameter which gives an idea about the quality of healing.

S. No	Suture	Antimicrobial assay (Zone of Inhibition in cm)		Hemocompatibility assay(% haemolysis)	Cytotoxicity Assay (% cytotoxicity)
		E. coli	*S. aureus*		
1	Uncoated	-	-	1.2 ± 0.09	4.2 ± 0.81
2	CPGNPs	3.6 ± 0.9	4.2 ± 0.7	0.8 ± 0.04	5.4 ± 0.97

Table 5: Antimicrobial, hemocompatibility and cytotoxicity of coated sutures. All the data presented were mean SD of triplicates. No significant statistical difference was noted on comparison between groups.

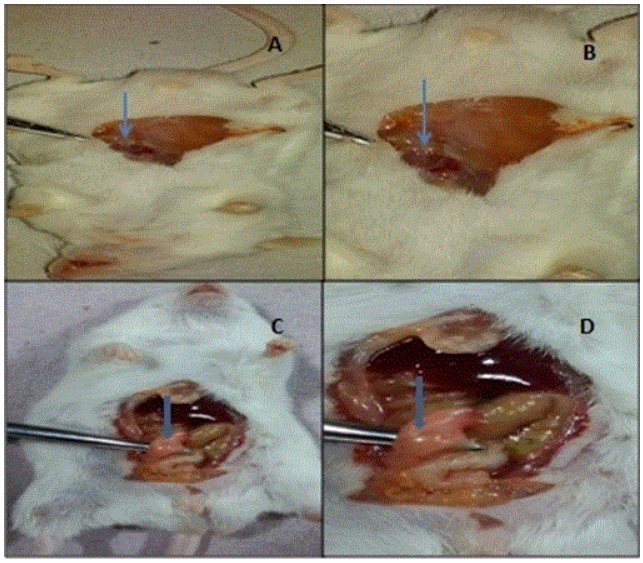

Figure 8: Picture showing the surgery in mice using drug coated sutures: A& B: 3rd day, C & D after 7th day of surgery.

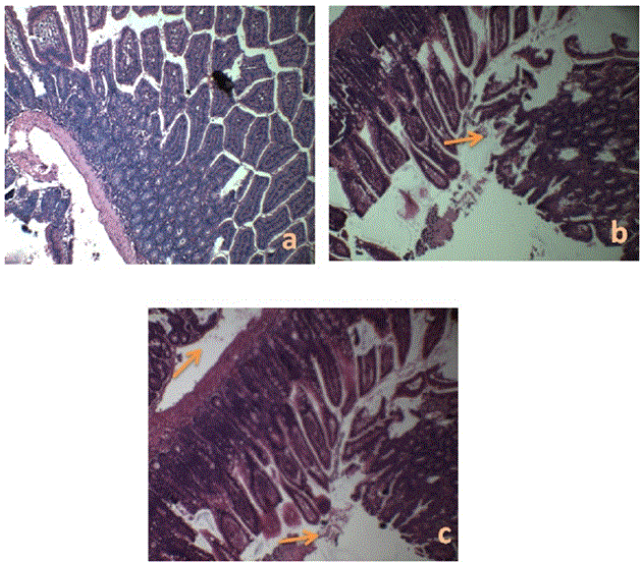

Figure 9: Histopathological sections of Intestinal anastomosis (Maginification 10 X, Magnification scale 50 μm), a: Normal Intestine section without any suture, b: Plain suture, c: CPCNP coated suture and Indicates → Inflammation and fibroblast infiltration.

The mean inflammatory cell infiltration and fibroblast deposition were presented in Table 6. The inflammatory scores were significantly lower with coated sutures in comparison with uncoated sutures which can be attributed to the well-known anti-inflammatory property of gold and curcumin used for coating sutures. But, the infiltration of fibroblasts was not much varying between the groups at the examined time point. Wound healing is majorly determined by the collagen and fibroblast levels which increase post 48 h of injury and reaches normalcy gradually as reported by Christensen et al. [47]. This indicates merit of further investigation at different time points will help understanding the process in a better way. From the present reports, we can summarize that anti-inflammatory property of the drug in coated sutures promoted fewer adhesions and better healing in the studied groups.

S. No	Suture	Adhesion score	Inflammatory cell infiltration	Fibroblast infiltration
1	Uncoated	3.2 ± 0.81	3.65 ± 0.27	1.6 ± 0.9
2	CPGNPs	0.8 ± 0.11*	0.72 ± 0.21*	1.2 ± 0.5

Table 6: *In vivo* study–Adhesion and histopathological score. All the data presented were mean ± SD of 8 observations. *: $p<0.05$ on comparison with uncoated group.

Conclusion

In the present work, curcumin colloidal gold NPs were prepared by wet-solvent precipitation method with 2:1 ratio using polyethylene glycol methyl thiol ether as a carrier. The prepared gold nanoparticles were coated onto the surface of absorbable suture. The particle size and PdI were measured for blank gold nanoparticles, thiolated PEG gold nanoparticles and curcumin colloidal gold nanoparticles. The particle size and PdI was significantly affected by varying the concentration of gold and reducing agent. Curcumin colloidal gold nanoparticles coating on suture was done by a slurry dipping method to improve the antibacterial property. The coated sutures showed an excellent antibacterial activity against gram positive and gram negative bacteria and drug release was observed up to 4 days. *In vivo* studies proved that coated sutures healed the tissue faster as compared to uncoated sutures. Hence it is concluded that the drug loaded sutures are quite suitable for preventing surgical site infections. The clinical usage of the present work should be explored in clinical trials for nosocomial infections and antimicrobial property of the coated sutures with different broad spectrum antibiotics can be explored.

Conflict of Interests

The authors declare that there is no conflict of interests regarding the publication of this paper.

Acknowledgement

The authors would like to thank DST-SERB for funding the project with sanction no: SB/EMEQ-019/2013. Dr. S. Chandrasekhar, Project Director, Dr. Sanjeeva Reddy, Registrar, NIPER, Hyderabad for providing facilities for the research.

References

1. Adekogbe I, Ghanem A (2005) Fabrication and characterization of DTBP-crosslinked chitosan scaffolds for skin tissue engineering. Biomaterials 26: 7241-7250.
2. Edlich RF, Panek PH, Rodeheaver GT, Turnbull VG, Kurtz LD, et al. (1973) Physical and chemical configuration of sutures in the development of surgical infection. Ann Surg 177: 679-688.
3. Sezer AD, Cevher E (1992) Biopolymers as Wound Healing Materials: Challenges and New Strategies. Biomater Appl Nanomed, pp: 383-414.

4. Gottrup F (2001) A New Concept of a Multidisciplinary Wound Healing Center and a National Expert Function of Wound Healing. Arch Surg 136: 765.
5. Li Y, Kumar KN, Dabkowski JM, Corrigan M, Scott RW, et al. (2012) New bactericidal surgical suture coating. Langmuir 28: 12134-12139.
6. Deliaert AE, Van den Kerckhove E, Tuinder S, Fieuws S, Sawor JH, et al. (2009) The effect of triclosan-coated sutures in wound healing. A double blind randomised prospective pilot study. J Plast Reconstr Aesthet surg 62: 771-773.
7. Mingmalairak C (2011) Antimicrobial sutures: new strategy in surgical site infections. Sci Against Microb Pathog Commun Curr Res Technol Adv: 313-323.
8. Chen QZ, Blaker JJ, Boccaccini AR (2006) Bioactive and mechanically strong Bioglass-poly(D,L-lactic acid) composite coatings on surgical sutures. J Biomed Mater Res Part B, Appl Biomater 76: 354-363.
9. He CL, Huang ZM, Han XJ (2009) Fabrication of drug-loaded electrospun aligned fibrous threads for suture applications. J Biomed Mater Res Part A 89: 80-95.
10. Asri LATW, Crismaru M, Roest S, Chen Y, Ivashenko O, et al. (2014) A Shape-Adaptive, Antibacterial-Coating of Immobilized Quaternary-Ammonium Compounds Tethered on Hyperbranched Polyurea and its Mechanism of Action. Adv Funct Mater 24: 346-355.
11. Dubas ST, Wacharanad S, Potiyaraj P (2011) Tunning of the antimicrobial activity of surgical sutures coated with silver nanoparticles. Colloids Surf A Physicochem Eng Asp 380: 25-28.
12. Augustine R, Rajarathinam K (2012) Synthesis and characterization of silver nanoparticles and its immobilization on alginate coated sutures for the prevention of surgical wound infections and the *in vitro* release studies. Int J Nanodimens 2: 205-212.
13. Gupta R, Pradesh U (2013) Nano-structured herbal antimicrobials. Int J Pharm Sci Res 4: 2028-2034.
14. Steinstraesser L, Hirsch T, Schulte M, Kueckelhaus M, Jacobsen F, et al. (2012) Innate defense regulator peptide 1018 in wound healing and wound infection. PLoS One 7: 39373.
15. Bell IR, Schwartz GE, Boyer NN, Koithan M, Brooks AJ (2013) Advances in Integrative Nanomedicine for Improving Infectious Disease Treatment in Public Health. Eur J Integr Med 5: 126-140.
16. Allahverdiyev AM, Kon KV, Abamor ES, Bagirova M, Rafailovich M (2011) Coping with antibiotic resistance: combining nanoparticles with antibiotics and other antimicrobial agents. Expert Rev Anti-infec Ther 9: 1035-1052.
17. Chamundeeswari M, Sobhana SSL, Jacob JP, Kumar MG, Devi MP, et al. (2010) Preparation, characterization and evaluation of a biopolymeric gold nanocomposite with antimicrobial activity. Biotechnol Appl Biochem 55: 29-35.
18. Freire-Moran L, Aronsson B, Manz C, Gyssens IC, So AD, et al. (2011) Critical shortage of new antibiotics in development against multidrug-resistant bacteria-Time to react is now. Drug Resist Updat 14: 118-124.
19. Vigderman L, Zubarev ER (2013) Therapeutic platforms based on gold nanoparticles and their covalent conjugates with drug molecules. Adv Drug Deliv Rev 65: 663-676.
20. Sardar R, Funston AM, Mulvaney P, Murray RW (2009) Gold nanoparticles: past, present, and future. Langmuir 25: 13840-13851.
21. Ravishankar Rai V, Jamuna Bai A(2011) Nanoparticles and their potential application as antimicrobials. Formatex, pp: 197-209.
22. Eustis S, El-Sayed MA (2006) Why gold nanoparticles are more precious than pretty gold: noble metal surface plasmon resonance and its enhancement of the radiative and nonradiative properties of nanocrystals of different shapes. Chem Soc Rev 35: 209-217.
23. Pissuwan D, Cortie CH, Valenzuela SM, Cortie MB (2010) Functionalised gold nanoparticles for controlling pathogenic bacteria. Trends Biotechnol 28: 207-213.
24. Anand P, Kunnumakkara AB, Newman RA, Aggarwal BB (2007) Bioavailability of Curcumin: Problems and Promises. Mol Pharm 4: 807-818.
25. Rodríguez-Carmona E, Villaverde A (2010) Nanostructured bacterial materials for innovative medicines. Trends Microbiol 18: 423-430.
26. Hatamie S, Nouri M, Karandikar SK, Kulkarni A, Dhole SD, et al. (2012) Complexes of cobalt nanoparticles and polyfunctional curcumin as antimicrobial agents. Mater Sci Eng C 32: 92-97.
27. Kakran M, Sahoo NG, Tan IL, Li L (2012) Preparation of nanoparticles of poorly water-soluble antioxidant curcumin by antisolvent precipitation methods. J Nanopart Res 14: 757.
28. Song Z, Feng R, Sun M, Guo C, Gao Y, et al. (2011) Curcumin-loaded PLGA-PEG-PLGA triblock copolymeric micelles: Preparation, pharmacokinetics and distribution *in vivo*. J Colloid Interf Sci, pp: 116-123.
29. Lin CC, Lin HY, Chen HC, Yu MW, Lee MH (2009) Stability and characterisation of phospholipid-based curcumin-encapsulated microemulsions. Food Chem 116: 923-928.
30. Gangwar RK, Dhumale VA, Kumari D, Nakate UT, Gosavi SW, et al. (2012) Conjugation of curcumin with PVP capped gold nanoparticles for improving bioavailability. Mater Sci Eng C 32: 2659-2663.
31. Manju S, Sreenivasan K (2012) Gold nanoparticles generated and stabilized by water soluble curcumin-polymer conjugate: Blood compatibility evaluation and targeted drug delivery onto cancer cells. J Colloid Interf Sci 368: 144-151.
32. Sahoo SK, Parveen S, Panda JJ (2007) The present and future of nanotechnology in human health care. Nanomed Nanotechnol Biol Med 3: 20-31.
33. Kokubo T, Kushitani H, Sakka S, Kitsugi T, Yamamuro T (1990) Solutions able to reproduce *in vivo* surface-structure changes in bioactive glass-ceramic A-W. J Biomed Mater Res 24: 721-734.
34. Gannu R, Vishnu YV, Kishan V, Rao YM (2007) Development of nitrendipine transdermal patches: *in vitro* and *ex vivo* characterization. Curr Drug Deliv 4: 69-76.
35. Furuzono T, Ishihara K, Nakabayashi N, Tamada Y (1999) Chemical modification of silk fibroin with 2-methacryloyloxyethyl phosphorylcholine I. Graft-polymerization onto fabric using ammonium persulfate and interaction between fabric and platelets. J Appl Polym Sci 73: 2541-2544.
36. Furuzono T, Ishihara K, Nakabayashi N, Tamada Y (2000) Chemical modification of silk fibroin with 2-methacryloyloxyethyl phosphorylcholine. II. Graft-polymerization onto fabric through 2-methacryloyloxyethyl isocyanate and interaction between fabric and platelets. Biomaterials 21: 327-333.
37. He Q, Zhang J, Shi J, Zhu Z, Zhang L, et al. (2010) The effect of PEGylation of mesoporous silica nanoparticles on nonspecific binding of serum proteins and cellular responses. Biomaterials 31: 1085-1092.
38. Lin YS, Haynes CL (2009) Synthesis and Characterization of Biocompatible and Size-Tunable Multifunctional Porous Silica Nanoparticles. Chem Mater 21: 3979-3986.
39. Stevens MG, Olsen SC (1993) Comparative analysis of using MTT and XTT in colorimetric assays for quantitating bovine neutrophil bactericidal activity. J Immunol Methods 157: 225-231.
40. Van der Ham AC, Kort WJ, Weijma IM, van den Ingh HF, Jeekel J (1991) Effect of fibrin sealant on the healing colonic anastomosis in the rat. Br J Surg 78: 49-53.
41. Ehrlich HP, Tarver H, Hunt TK (1973) Effects of vitamin A and glucocorticoids upon inflammation and collagen synthesis. Ann Surg 177: 222-227.
42. Ceran C, Aksoy RT, Gülbahar O, Oztürk F (2013) The effects of ghrelin on colonic anastomosis healing in rats. Clinic 68: 239-244.
43. Link S, El-Sayed MA (1999) Size and Temperature Dependence of the Plasmon Absorption of Colloidal Gold Nanoparticles. J Phys Chem B 103: 4212-4217.
44. Huang ZM, He CL, Yang A, Zhang Y, Han XJ, et al. (2006) Encapsulating drugs in biodegradable ultrafine fibers through co-axial electrospinning. J Biomed Mater Res Part A 77: 169-179.

45. Herricks TE, Kim SH, Kim J, Li D, Kwak JH, et al. (2005) Direct fabrication of enzyme-carrying polymer nanofibers by electrospinning. J Mater Chem 15: 3241.

46. Mannan A, Pawar SJ (2014) Anti-infective coating of gentamicin sulphate encapsulated PEG/PVA/chitosan for prevention of biofilm formation. Int J Pharm Pharm Sci 6: 571-576.

47. Christensen H, Chemnitz J, Christensen BC, Oxlund H (1995) Collagen structural organization of healing colonic anastomoses and the effect of growth hormone treatment. Dis Colon Rectum 38: 1200-1205.